NATIONAL ADVISORY COMMITTEE FOR AERONAUTICS

TECHNICAL NOTE 1939

THE EFFECTS OF AERODYNAMIC BRAKES UPON THE SPEED CHARACTERISTICS OF AIRPLANES

By Jack D. Stephenson

Ames Aeronautical Laboratory
Moffett Field, Calif.

Washington
September 1949

NATIONAL ADVISORY COMMITTEE FOR AERONAUTICS

TECHNICAL NOTE 1939

THE EFFECTS OF AERODYNAMIC BRAKES UPON THE SPEED CHARACTERISTICS OF AIRPLANES

By Jack D. Stephenson

SUMMARY

A study has been made of the factors influencing the performance of aerodynamic brakes. The requirements which must be met in order for the brakes to provide the necessary control over the forward speed are discussed for various flight conditions under which they may be used. Equations relating the speed and altitude are presented for several cases in which certain simplifying assumptions are made. For these cases, formulas and graphs in the report furnish a means of quickly computing the longitudinal speed variations, the dive angles, and the rates of descent for airplanes having known drag characteristics. For the cases to which the simplifying assumptions do not apply, it is indicated that a satisfactory solution, which takes into account all of the possible variables (such as atmospheric density, drag coefficient, and flight-path angle) can be obtained by a step-by-step method of calculation. Graphs are presented to reduce the time required for step-by-step calculations. Example calculations, which show each step in detail, illustrate the use of the graphs and formulas.

The increases in drag coefficient that are characteristic of several types of wing and fuselage aerodynamic brakes, which have been tested in wind tunnels or in flight, are summarized in the report. The effect of Mach number on the drag coefficient and the effect of partial brake deflection are included where such data are available.

INTRODUCTION

The continued improvement in the aerodynamic design of high-speed airplanes has brought the normal operating speeds near to their maximum safe speeds. As a result of low drag and of high engine output, airplanes may under certain circumstances accelerate to speeds at which dangerous compressibility effects or structural loadings arise. The trend toward higher wing loadings has added considerably to the possibility of attaining dangerous speeds, especially at the high operating altitudes which are characteristic of many modern airplanes.

One means of controlling speed is the use of aerodynamic brakes. This report is concerned with the problem of relating the drag increases due to aerodynamic brakes to the control of forward speed. Problems of buffeting, of changes in stability, of aerodynamic loads, and of changes in trim, which may arise when a particular brake is used on an airplane, are not considered. If a satisfactory brake is to be selected for an airplane, however, the possible occurrence of such phenomena must be investigated for the airplane and brake combination.

The increases in drag that result from the use of air brakes have been measured in wind-tunnel and flight tests for a large variety of brakes. In this report a summary of such drag data is presented. The effect of increases in the drag coefficient upon the speed variation calculated for a hypothetical airplane is illustrated. A procedure for calculating the speed of an airplane at any point in arbitrarily specified maneuvers is presented and discussed.

SYMBOLS

C_{D_n} net drag coefficient $\left(\frac{D_n}{qS}\right)$

ΔC_D increase in drag coefficient due to the aerodynamic brake $\left(\frac{\text{brake drag}}{qS}\right)$

ΔC_{D_B} drag coefficient due to the aerodynamic brake referred to the area of the brake $\left(\frac{\text{brake drag}}{qS_B}\right)$

C_L lift coefficient $\left(\frac{\text{lift}}{qS}\right)$

D_n algebraic sum of aerodynamic forces parallel to the direction of flight, positive toward the rear, pounds

K deceleration factor $\left(\frac{1}{2}\frac{\rho g}{W/S} C_{D_n}\right)$, per foot

M Mach number

S wing area, square feet

S_B maximum projected area of the aerodynamic brake, including slots, gaps, and perforations, square feet

V	true airspeed, feet per second
V_V	vertical component of speed, feet per minute
ΔV	speed change in time interval Δt, feet per second
$\overline{V}$	average speed during time interval Δt, feet per second
W	airplane weight, pounds
W/S	wing loading, pounds per square foot
a	longitudinal acceleration, feet per second squared
$\overline{a}$	average longitudinal acceleration during time interval Δt, feet per second squared
b	wing span, feet
g	acceleration due to gravity, feet per second squared
h	altitude, feet
Δh	altitude change in time interval Δt, feet
n	indicated normal acceleration factor $\left(\frac{\text{indicated acceleration normal to flight path}}{g}\right)$
q	dynamic pressure $\left(\frac{1}{2}\rho V^2\right)$, pounds per square foot
r	radius of curvature of flight path, feet
t	time, seconds
Δt	time increment, seconds
α	angle of attack, degrees
γ	flight-path angle from the horizontal (positive for a climb), degrees
$\Delta\gamma$	change in flight-path angle in the time interval Δt, degrees
$\overline{\gamma}$	average flight-path angle during the time interval Δt, degrees
ρ	air density, slugs per cubic foot

Subscripts

e estimated

o value at $t = 0$

1 value at beginning of time interval Δt

CONTROL OF AIRPLANE SPEED

Flight experience has indicated that the control of forward speed, which is possible through the use of aerodynamic brakes, is of considerable value in the operation of airplanes of all types. The required action of brakes in controlling the speed differs among various airplanes, and for any one airplane the requirements may differ with the type of maneuver that is to be performed. For the purpose of the present discussion, brakes are considered according to their use in producing longitudinal deceleration at approximately constant altitude, in permitting greater angles of dive at moderately low speeds, and in avoiding dangerously high speeds.

Deceleration at Constant Altitude

It is to be expected that a device that controls the longitudinal deceleration would find especial applications in the operation of combat airplanes. A sudden deceleration would be required in order for a fighter airplane which was overtaking its target to slow down so as to have a maximum amount of time for firing. Rapid decelerations may also be called for in traffic-control zones during poor visibility in order to prevent collision.

Aerodynamic brakes may assist the pilot in performing various maneuvers. If the maximum normal acceleration is fixed by the maximum to which the pilot may be subjected or by structural limitations of the airplane, the minimum radius of curvature of the flight path varies with the square of the speed. Thus, a reduction in speed by the use of air brakes prior to and during a maneuver would effect a substantial decrease in the minimum turning radius.

The performance of aerodynamic brakes used primarily for speed reduction is indicated by the magnitude of the longitudinal deceleration in level flight. Calculations showing the variation of speed with time can be used to measure the comparative suitability of different brakes on the same airplane in producing needed changes of speed.

Speed Control in Dives

Aerodynamic brakes which keep the speed moderately low during dives are needed for the performance of some tactical maneuvers. For the dive bomber, low speed is required as a precaution against excessive normal accelerations during pull-outs at low altitude. In rapid descent of large airplanes, the desirability of avoiding high forward speeds is apparent. The braking which would be sufficient to prevent increases in speed may be used to gauge the performance of brakes for airplanes in controlled-speed dives. Aerodynamic data for brakes to be used on airplanes in such dives may be evaluated by a comparison of the measured brake drag with the brake drag which would be required to reduce the longitudinal acceleration to zero.

Speed Control at High Speed

The maximum safe diving speed is commonly specified as the maximum indicated airspeed upon which calculations of loads are based in the structural analysis. The rapid change in altitude resulting from a steep dive at high speed means that the true speed would have to be reduced in order to keep from exceeding the allowable indicated speed. Calculations which show the variation with time of the speed of an airplane with brakes indicate whether the drag of the brakes is sufficient to produce the required reductions in speed. Methods are presented in this report to aid in making such calculations.

One of the most important examples of the employment of aerodynamic brakes is their use in avoiding dangerous compressibility effects. These effects take the form of changes in longitudinal stability, such as described in reference 1, or as other erratic behavior of airplanes or their controls. Without brakes, pilots of modern high-speed combat airplanes are not always able to avoid speeds at which such compressibility effects appear.

A method of calculation which shows the variation with time of speed and altitude of an airplane throughout various maneuvers can be used to determine whether the aerodynamic brakes are adequate to keep the maximum Mach number below a certain critical value.

ANALYSIS

The foregoing discussion has indicated various instances wherein a need for aerodynamic brakes has been observed. The drag increments due to air brakes do not by themselves afford a complete measure of the degree to which brakes meet these needs. Brake designs can be evaluated by studies which demonstrate the effects of the brakes upon the forward speed of airplanes. These effects are analyzed in this

report through a study of equations of longitudinal motion of airplanes, of the validity of various initial assumptions, and of the accuracy of approximate calculations.

Algebraic Analysis

The deceleration of an airplane with air brakes depends upon a number of factors, such as variations of flight-path angle, of altitude, and of speed, as well as upon the characteristics of the brakes themselves. In order to separate the effects of the brakes from the other effects, the problem is simplified by assuming that one or more of these factors is constant. The effects of various air-brake designs and locations on the variation of speed with time may then be readily determined. The following sections present analyses employing such simplifications.

Level-flight deceleration.- In level flight, one form of the equation of longitudinal motion of an airplane is

$$\frac{dV}{dt} = -\frac{g}{W} D_n \tag{1}$$

where D_n is the algebraic sum of the aerodynamic forces acting parallel to the flight direction, positive being taken toward the rear. The value of D_n is affected by any changes in the drag of the airplane, which may result, for example, from variations in angle of attack, variations of Mach number, or changes in the setting of the air brakes. Any factors that cause the thrust to change, such as variations in engine output, variations in propeller efficiency, and effects of velocity upon propeller or engine thrust also influence D_n. It is convenient to express D_n in the form of a force coefficient

$$C_{D_n} = \frac{D_n}{\frac{1}{2}\rho V^2 S}$$

Substituting in equation (1),

$$\frac{dV}{dt} = -C_{D_n} \frac{\rho}{2} \frac{gV^2}{W/S}$$

If C_{D_n} is constant, this expression may be integrated to give

$$V = \frac{1}{Kt + (1/V_o)} \tag{2}$$

where

$$K = C_{D_n} \frac{\rho}{2} \frac{g}{W/S}$$

The quantity K is a measure of the effects of altitude, wing loading, and net drag coefficient upon the longitudinal acceleration and in this report is referred to as the "deceleration factor." The value of the deceleration factor may be obtained for an airplane from figure 1(a), which takes into account the effects of altitude and of wing loading, and figure 1(b) which includes the effect of the net drag coefficient.

The velocity variation given by equation (2) has been plotted in figure 2 for four initial speeds: 300, 500, 700, and 900 feet per second. Curves are given for various values of deceleration factor K. Comparison of the slopes of curves for equal values of K shows a considerable increase in the deceleration as the initial speed increases.

In deriving equation (2), it was assumed that C_{D_n} was constant during the time interval considered. For this assumption to be valid, the engine output must be constant and the effects of speed changes on the thrust and drag coefficients must be negligible. If aerodynamic brakes are extended at the start of the time interval, the resulting increase in drag must be so rapid that it can be approximated by an instantaneous increase.

It is obvious that assuming C_{D_n} (or K) constant will in some cases lead to large errors. However, the results can represent the actual velocity variations fairly accurately under certain conditions. Below the Mach number of drag divergence the variation of airplane drag coefficient with Mach number is generally small. The effect of a delay due to the time required for full extension of the air brakes could introduce a large discrepancy; however, a rapid rate of extension is an essential characteristic of brakes which are to be used at high speeds.

It is possible to express variations in C_{D_n} as a series of instantaneous changes occurring at chosen time intervals during the deceleration. The variation of speed with time is then given by equation (2) with values of K computed for each interval and values of V_o successively determined as the velocity at the end of each preceding interval. The same variation may be obtained from figure 2 by shifting along the time axis portions of the curves having these values of deceleration factor and initial velocity. The curve thus obtained is continuous but changes slope abruptly at the start of each interval.

Constant flight-path inclination.— When the flight path is inclined, the component of weight W parallel to the direction of motion must be included, and the equation is

$$\frac{dV}{dt} = \frac{g}{W} \left(-D_n - W \sin \gamma\right)$$

where γ is the flight-path angle, positive for climbing flight. Substituting K as in the case of level flight,

$$\frac{dV}{dt} = -KV^2 - g \sin \gamma \tag{3}$$

The assumption can again be made that K does not vary during the period of time being considered. Then (as shown in reference 2) equation (3) integrates as follows to give the velocity variation for an airplane in a dive or climb at a constant angle:

If γ is negative and $\sqrt{L/K} < V_o$, where $L = -g \sin \gamma$

$$V = \sqrt{L/K} \coth \left[\sqrt{L/K} \, (Kt + C_1)\right] \tag{4}$$

where

$$C_1 = \frac{1}{2} \sqrt{K/L} \log_e \frac{V_o\sqrt{K} + \sqrt{L}}{V_o\sqrt{K} - \sqrt{L}}$$

If $\sqrt{L/K} > V_o$,

$$V = \sqrt{L/K} \tanh \left[\sqrt{L/K} \, (Kt + C_2)\right] \tag{5}$$

where

$$C_2 = \frac{1}{2} \sqrt{K/L} \log_e \frac{\sqrt{L} + V_o\sqrt{K}}{\sqrt{L} - V_o\sqrt{K}}$$

If γ is positive,

$$V = N \cot \left[N \, (Kt + C_3)\right] \tag{6}$$

where

$$N = \sqrt{-L/K}$$

and

$$C_s = \frac{1}{N} \cot^{-1} (V_o/N)$$

In assuming that K is constant the same approximations are made as in the case of level flight, together with the additional assumption that the density does not vary as a result of the inclined flight. It is necessary to estimate an average value of density, and, for large changes in altitude, some improvement in accuracy can be gained by dividing the time under consideration into shorter intervals and making separate calculations for each interval.

Constant-speed dive.- If there is adequate control over the drag, an airplane can be dived at any angle at constant speed. Such control requires a net drag coefficient given by the relation

$$C_{D_n} = -\frac{2(W/S)\sin \gamma}{\rho V^2}$$

For most airplanes having even moderately high wing loadings and low drag, however, it is not feasible to provide air brakes effective enough to prevent increases in speed under all conditions. The combination of factors which govern the maximum angle for a constant-speed dive can be determined from figure 3. This figure shows the relation between forward speed, angle of dive, and rate of descent. The other variables which affect the dive, such as altitude, net drag coefficient, and wing loading, are again included in the single quantity K. Figure 3, used in conjunction with figures 1(a) and (b), permits graphical solution for any one of these quantities when equilibrium exists.

An indication of the separate effects of altitude and speed upon the net drag required for equilibrium is given in figure 4. Wing loadings of 30 and 50 pounds per square foot were assumed. On the left in figure 4 the drag coefficient is plotted against altitude for a vertical dive. It is apparent that unless the airplane speed is very high, the equilibrium drag coefficient is large even at low altitudes and becomes extremely large at high altitudes. On the right in figure 4, curves of constant drag coefficient are plotted against the dive angle. The drag coefficient as a function of altitude and airspeed may be found for any dive angle by reading C_{D_n} corresponding to the ordinate from the left part of the figure at the desired value of dive angle.

Graphical Analysis

As the number of variables in the equation of motion is increased, it becomes impractical to obtain an accurate solution by direct integration of the equation of motion along the flight path. Because of the arbitrary manner in which some of the quantities involved can be varied, a method of calculation in which specific variations of these quantities are assumed would place untenable restrictions on the usefulness of the solution. Among the quantities which cannot be defined mathematically by expressions suitable for all problems are the following:

(a) Variation of engine output with time

(b) Variations of drag and thrust with Mach number

(c) Variation of flight-path angle with time

(d) Variation of drag with lift

(e) Variation of drag with time when the air brakes are operated

These variations, which are either arbitrary or empirical, and the variation of atmospheric density with time can all be taken into account if the calculations are made by graphical means. The calculations can be performed by a step-by-step method in which the longitudinal acceleration in each step is obtained from graphs that have been prepared. The change in velocity can then be ascertained as the integral of the acceleration with respect to time. This integral may be evaluated graphically, but it has been found that the integration is sufficiently accurate if trapezoidal elements of area are assumed and an arithmetical evaluation is used.

Constant flight-path inclination.- The longitudinal acceleration (or deceleration) at the beginning of the interval of time being studied is determined by the known or assumed initial flight conditions. The acceleration at any later time, however, cannot be computed directly, since it is a function of speed and altitude, the values of which are not known. This acceleration may be found by dividing the total time interval into a series of increments and calculating, step by step, the conditions at the end of each increment. The step-by-step calculation is made by estimating the speed and altitude at the end of each increment upon the basis of the known conditions at the beginning of that increment. With these estimated values, the longitudinal acceleration at the end of the increment may be computed. The speed and altitude at this time may then be calculated to greater accuracy and compared with the estimated values. Although this procedure amounts to a method of successive approximations, it has been found that the

velocity and altitude can usually be estimated so accurately that the first approximation is sufficient. If it is not, a second approximation may be made, or else smaller increments of time can be chosen. The time increments should be small enough so that all important changes in acceleration are taken into account, but large enough to keep the number of steps to a minimum.

The change in altitude during the time Δt for flight with a constant flight-path angle is

$$\Delta h = \overline{V} (\Delta t) \sin \gamma \tag{7}$$

where $\overline{V}$ is the average velocity. The estimated altitude change for each Δt is given by this relation in which $\overline{V}$ is the average velocity estimated for that incremental time.

The longitudinal acceleration at the end of the time increment is given by figure 1, which includes the effects of altitude and wing loading (fig. 1(a)), of drag coefficient (fig. 1(b)), of velocity (fig. 1(c)), and of flight-path inclination (fig. 1(d)). When the speed variation of an airplane at a constant flight-path inclination is being calculated, the values of flight-path angle and wing loading are known. The altitude and speed are estimated, as indicated in the preceding paragraphs. The net drag coefficient, which may be a function of the flight Mach number and the airplane lift coefficient, is obtained from experimental or theoretical data using values of Mach number and lift coefficient computed from the estimated speed and altitude.

The increase or decrease in velocity during the time Δt, assumed to be given by the area of the trapezoidal element under the curve of acceleration against time, is

$$\Delta V = \frac{1}{2} (a_1 + a) \Delta t$$

in which a_1 and a are the longitudinal acceleration at the beginning and of the end of the time increment. The velocity and Mach number which result from this velocity change can now be compared with the estimated values to ascertain whether the estimates are accurate.

Variable flight-path inclination.- Because proposed aerodynamic brakes are to be designed for use in flight at any time, a method for calculating the speed of an airplane during any flight evolution is needed. The calculations for a dive at constant angle discussed in the preceding section would not accurately represent a steep dive of a

high-speed airplane because a large part of the latter maneuver would consist of the dive entry and pull-out. The effects of curvature of the flight path can be evaluated by an extension of the graphical method just described.

When the airplane is following a path of increasing or decreasing inclination, a calculation of the changes in altitude is complicated by the necessity of extrapolating along the curved path. One means of making such an extrapolation is to assume that the airplane follows a path consisting of a series of circular arcs. The curvature of the flight path, which is a function of the forces normal to the direction of motion, is evident to the pilot as a normal acceleration. In order to permit the changes in altitude to be expressed as a function of the normal acceleration felt by the pilot, motion in a vertical plane is first considered. The altitude change during the period of time Δt can be computed by the relation

$$\Delta h = r \left[\cos \gamma_1 - \cos (\gamma_1 + \Delta\gamma)\right] \tag{8}$$

where r is the radius of the arc of the flight path, γ_1 is the flight-path angle at the beginning of the period, and $\Delta\gamma$ is the angular change in the direction of motion during the time Δt.

The actual acceleration normal to the direction of flight is equal to the indicated normal acceleration minus the normal acceleration due to the weight of the airplane. If n is the indicated normal acceleration factor,

$$\frac{V^2}{r} = g (n - \cos \gamma) \tag{9}$$

In figure 5(a) the acceleration factor n is plotted against the quantity $(n-\cos \overline{\gamma})$ for values of $\overline{\gamma}$ from 0° to 90°. The curves for negative values of $\overline{\gamma}$ are the same as for positive values. Figure 5(b) presents the variation of airspeed with $(n-\cos \overline{\gamma})$ for constant radii of flight-path curvature. Example guide lines show how the radius may be found by projecting the abscissa from a point in figure 5(a) to the line for $\cos \overline{\gamma} = 0$ ($\overline{\gamma} = 90^\circ$, positive n) and continuing at this ordinate to the desired value of average airspeed in part (b).

Figures 5(c) and 5(d) give a graphical solution for $\Delta\gamma$ as a function of $(n - \cos \overline{\gamma})$, $\overline{V}$, and Δt. The graphs were obtained from the following equations. Since r is considered to be constant during the time interval Δt,

$$\frac{1}{57.3}\frac{d\gamma}{dt} = \frac{V}{r}$$

Substituting $\frac{V}{r}$ from equation (9),

$$\frac{d\gamma}{dt} = 57.3\ g\ \frac{n - \cos\gamma}{V}$$

from which, by using small finite time intervals, $\Delta\gamma$ may be computed as

$$\Delta\gamma = \frac{d\gamma}{dt}\Delta t$$

The estimated average speed $\overline{V}_e$ during the time Δt is used in calculations for radius of curvature and $d\gamma/dt$. In addition, an estimate of the average flight-path inclination is necessary to determine the value of the abscissa $(n-\cos\overline{\gamma})$. The accuracy of this estimate can be checked as soon as $\Delta\gamma$ has been found, if it is assumed that $\overline{\gamma}$ is the initial angle plus half the increment.

Figure 5(f) shows the variation with $\Delta\gamma$ of the quantity $[\cos\gamma_1 - \cos(\gamma_1 + \Delta\gamma)]$. There are two sets of values of γ_1 identifying the curves, one of which applies when $\Delta\gamma$ is positive and one when $\Delta\gamma$ is negative. This dual labeling is used because the curves have been plotted on only one side of the vertical axis. The algebraic sign of $\Delta\gamma$ may readily be ascertained since it is the same as the sign of the quantity $(n-\cos\gamma)$. When the ordinate of figure 5(f) and the radius of flight-path curvature, figure 5(b), are known, the change in altitude is given by figure 5(e). Although the algebraic sign of the change in altitude is not shown in the graph, in most cases it is evident from the problem. If the sign is not apparent, a simple diagram showing γ_1 and $\Delta\gamma$ will indicate whether the altitude increases or decreases during the time Δt.

It is seen that figure 5 cannot be used when the flight-path radius becomes very large. In this case the altitude change may be calculated with sufficient accuracy from equation (7).

The graphical solution for the change in altitude is arranged so as to be used directly with maneuvers in a vertical plane which are identified by the magnitude of the normal acceleration or load factor. For maneuvers not wholly in a vertical plane, part of the total load factor results from accelerations in a horizontal direction and does not affect the altitude. In this case the value of the load factor to

be used with the graphs is the component measured normal to the flight path in a vertical plane tangent to the flight path.

The procedure in the calculation of the speed changes within each time increment is the same with a variable flight-path angle as with a constant angle. The flight-path angle and the altitude are progressively evaluated for the beginning of each time interval and their values are estimated for the interval by the method just described. The acceleration of the end of the increment Δt is obtained graphically (fig. 1) and the velocity is computed. Step-by-step calculations furnish the velocity variation during the complete interval being investigated.

DRAG CHARACTERISTICS OF AERODYNAMIC BRAKES

The characteristics of various aerodynamic brakes have been investigated in wind-tunnel and flight tests. (See references 3 through 7.) Results of such tests are summarized in this report. Data are presented in the form of increments in drag coefficient which are attributable to the brakes. It is to be expected that in some cases such increments are affected by the particular location of the brakes on the wing, the fuselage, or elsewhere, and by their proximity to other components of the airplane. The air brakes shown are representative of installations in which air brakes are added to typical fuselages or at different locations on wings.

Geometric data and incremental drag coefficients for the aerodynamic brakes shown in figure 6 are presented in table I. These data indicate increments in the drag of the airplane which are small in comparison with the values required in a steep dive for an airplane having a moderate wing loading (fig. 4). Increased drag can be obtained by increasing the relative size of the brake. However, increasing the size is practical only within the limitations of available space into which the brake may be retracted. The size is limited also by considerations of weight of the structure transmitting the aerodynamic loads, and by the effects of large brakes upon the trim, stability, and buffeting of the airplane.

Table I indicates that the drag coefficients (based upon the areas of the air brakes) vary over a wide range, depending upon the shape and location of the brake on the airplane. The lowest drag coefficient was measured for the picket-fence type of brake (type N). This low value of brake drag coefficient might be expected since the brake area used as a reference is more than twice the actual frontal area. The highest drag resulted from solid brakes at forward positions on the wing (types F and G). This forward location of the brakes results in a spoiling action which causes changes in the lift as well as drag. Since the drag increments in table I are for zero lift, a part of the

drag is attributable to the change in angle of attack necessary for the lift to be constant. Because the rate of change of drag with angle of attack for lift coefficients near zero is small, the effect of such an angle-of-attack change is not large for the data presented. Apparently, therefore, the large drag values of the spoiler-type brakes result from changes in the flow over the wing.

From the discussion of the functions of aerodynamic brakes, it is evident that they should be designed to be effective throughout a wide range of conditions. There should be a smooth increase in drag as the brake is extended, permitting any position between fully open and closed to be selected with a corresponding control over the deceleration. The variations of drag coefficient with percent extension for brakes of several types are shown in figure 7.

The effect of Mach number upon air-brake drag is dependent upon the particular installation. The variations of incremental drag coefficient with Mach number for two aerodynamic brakes (of type D) on a rectangular wing are shown in figure 8. The drag characteristics are affected to a large extent by the lift on the wing. At an angle of attack of -1.0°, the rate of rise of drag with Mach number became greater as the Mach number increased from 0.3 to 0.775. At an angle of attack of 3.0°, the drag increased with Mach number up to a Mach number of 0.7 and then began to decrease. The drag coefficient due to the fuselage side brake, shown in figure 8, increased nearly uniformly with Mach number throughout the range of Mach numbers from 0.3 to 0.875. The drag coefficient due to the fuselage dive-recovery flaps (type P) increased rapidly with Mach number above 0.6, rising to 161 percent of its low-speed value at a Mach number of 0.8.

EXAMPLE CALCULATIONS

Examples are presented to illustrate the procedures for calculating the variations with time of the forward speed and altitude. These calculations are for an airplane with a wing loading of 50 pounds per square foot, initially flying at a true airspeed of 700 feet per second. An initial altitude of 25,000 feet was assumed and some additional calculations were made assuming an initial altitude of 10,000 feet to indicate the effects of this reduction in altitude.

The longitudinal aerodynamic forces on the airplane can be represented by the coefficient

$$C_{D_n} = C_{D_A} + C_{D_T} + FC_L^2 + \Delta C_D$$

where the terms are defined as follows:

C_{D_A} drag coefficient of the airplane without air brakes, excluding the induced drag

C_{D_T} force coefficient, either drag or thrust, due to the propulsion unit

F induced drag factor

ΔC_D increment in drag coefficient resulting from the extension of aerodynamic brakes

Level Flight

The speed variation for level flight is given by equation (2) in which it is necessary that C_{D_n} be constant.

The following coefficients have been assumed:

$$C_{D_A} + C_{D_T} = 0.013$$

$$F = 0.060$$

$$FC_L^2 = 0.001$$

$$\Delta C_D = 0.100$$

$$C_{D_n} = 0.114$$

For an altitude of 25,000 feet,

$$K = C_{D_n} \frac{\rho}{2} \frac{g}{W/S}$$

$$= (0.114) \frac{0.001066}{2} \left(\frac{32.2}{50}\right) = 0.0391 \times 10^{-3} \text{ per foot}$$

$$V = \frac{1}{Kt + (1/V_o)} = \frac{25{,}600}{t + 36.6}$$

For an altitude of 10,000 feet

$$K = 0.0644 \times 10^{-3} \text{ per foot}$$

$$V = \frac{15{,}500}{t + 22.2}$$

The relations for speed as a function of time are shown in figure 9 for level flight. Figure 9 indicates that, by reducing the altitude from 25,000 to 10,000 feet, the time required for a given speed reduction is decreased by 40 percent.

Constant Dive Angle

The variation of speed with time during the first 15 seconds for a constant-angle dive has been calculated for the same assumed coefficients. A dive angle of 60° was assumed.

Initial altitude, 25,000 feet

Estimated average altitude, 20,500 feet

$K = 0.0000458$ per foot (fig. 1(b))

$L = -g \sin \gamma = (32.2)\ (0.866) = 27.9$ feet per second squared

$\sqrt{L/K} = 780.5$ feet per second

Since $\sqrt{L/K}$ is greater than V_o, equation (5) is used.

$$C_2 = \frac{1}{2} \sqrt{K/L} \log_e \frac{\sqrt{L} + V_o \sqrt{K}}{\sqrt{L} - V_o \sqrt{K}} = 0.001866$$

$$V = 780.5 \tanh [780.5\ (0.0000458t + 0.001866)]$$

Initial altitude, 10,000 feet

Average altitude, 5,000 feet

$K = 0.0000752$ per foot

$\sqrt{L/K} = 609$ feet per second

Since $\sqrt{L/K}$ is less than V_o, equation (4) is used.

$$V = 609 \coth [609(0.0000752t + 0.002187)]$$

The relations for speed as a function of time when the airplane is in a 60° dive are shown in figure 9.

A more accurate solution results from a step-by-step calculation. The velocity relations have been calculated by this method for comparison with the relations given by the equations. In order for the results of the step-by-step calculations to be comparable to the formulas, the assumption is again made that there is no variation in C_{D_n}. However, the effect of the variation in density is included, instead of assuming an average value. The step-by-step calculations for an initial altitude of 25,000 feet are presented in table II and the results of the calculations are shown in figure 9.

Calculations were made also to indicate the effect of a lag in the time for the drag due to the air brakes to reach its full value. It was assumed that the increase in drag caused by extending the brakes takes place during the interval between 1 and 2 seconds after the brake actuation is started. The amount by which the curve is displaced (fig. 9) indicates the gain in braking effect that can be realized by designing the brakes for minimum delay in opening.

It is seen from the slopes of the velocity curves in figure 9 that a change in flight-path angle from level flight to a dive of 60° results in a change from an initial deceleration of 18 feet per second squared to an initial acceleration of 6.8 feet per second squared for the assumed airplane with aerodynamic brakes at an altitude of 25,000 feet.

Entry Into a Dive

An example in which the flight-path angle is variable is provided in the calculations of the speed during a dive entry. The same initial speed, altitudes, and coefficients as in the preceding example are used.

It is assumed that the airplane is flown so that from level flight the indicated normal acceleration factor decreases to −1.5 within the first second and is then held constant until the airplane is in a 60° dive. The detailed calculations are presented in table III for an initial altitude of 25,000 feet. The results, plotted in figure 10, show the variation of longitudinal acceleration, dive angle, and speed with time for initial altitudes of 25,000 and 10,000 feet.

CONCLUDING REMARKS

Aerodynamic brakes afford a means of avoiding undesired increases in speed during the operation of an airplane, make possible rapid decelerations in flight, and allow a considerable increase in the angle of descent at constant speed. A measure of the utility of aerodynamic

brakes is provided by calculations which show how the speed of an airplane in a specified maneuver is altered by the employment of the air brakes.

Equations are presented in this report which permit a rapid calculation of the speed changes with time. Use of the equations results in close approximations to the values obtained by more accurate methods. The equations are not general, however, and apply only to several specific problems. The speed during a maneuver can be accurately calculated as a function of time by a step-by-step procedure. The graphs presented in this report substantially reduce the time required to make such calculations.

Ames Aeronautical Laboratory,
National Advisory Committee for Aeronautics,
Moffett Field, Calif., May 31, 1949.

REFERENCES

1. Hood, Manley J., and Allen, H. Julian: The Problem of Longitudinal Stability and Control at High Speeds. NACA Rep. 767, 1943.

2. Lowell, Arthur L: Fighter Airbrakes. Introductory Investigation of Means for Improving the Tactical Effectiveness of Combat Aircraft by Making Provisions for Rapid Decelerations in Flight. ACTR 4772 Army Air Corps, 1942.

3. Purser, Paul E., and Turner, Thomas R.: Aerodynamic Characteristics and Flap Loads of Perforated Double Split Flaps on a Rectangular NACA 23012 Airfoil. NACA ARR, Jan. 1943.

4. Purser, Paul E., and Turner, Thomas R.: Wind-Tunnel Investigation of Perforated Split Flaps for Use as Dive Brakes on a Tapered NACA 23012 Airfoil. NACA ARR, Nov. 1941.

5. Knowler, A. E., and Pruden, F. W.: The Effect of Brake Flaps on an Aerofoil at High Speeds. R.& M. No. 2211, June 1942.

6. Fuchs, D.: Wind-Tunnel Investigations of Diving Brakes. NACA TM 1033, Nov. 1942.

7. Laitone, Edmund V., and Summers, James L.: An Additional Investigation of the High-Speed Lateral-Control Characteristics of Spoilers. ACR 5D28, June 1945.

TABLE I.— SUMMARY OF THE DRAG CHARACTERISTICS OF VARIOUS AERODYNAMIC BRAKES[a]

[b] Brake type	Description	Airplane component tested with brake	Chordwise location of brake		Brake chord		Brake span		Brake angle		Brake area ratio, $\frac{S_B}{S}$	ΔC_D based on wing area	ΔC_D based on brake area	Remarks	Ref.
			Upper surface	Lower surface	Upper surface	Lower surface	Upper surface	Lower surface	Upper surface	Lower surface					
A	Perforated split flaps	Rectangular wing	[c] 0.80c	0.80c	0.200c	0.200c	$0.600\frac{b}{2}$	$0.600\frac{b}{2}$	90°	90°	0.2400	0.243	1.01	---	3
A	Perforated split flaps	Rectangular wing	.80c	.80c	.200c	.200c	$1.000\frac{b}{2}$	$1.000\frac{b}{2}$	90°	90°	.4000	.414	1.03	---	3
B	Perforated split flaps	Tapered wing	[d] .80$\bar{c}$	.80$\bar{c}$	.200$\bar{c}$	.200$\bar{c}$	$.600\frac{b}{2}$	$.600\frac{b}{2}$	60°	60°	.2400	.190	.79	---	4
B	Perforated split flaps	Tapered wing	.80$\bar{c}$	.80$\bar{c}$	.200$\bar{c}$	.200$\bar{c}$	$1.000\frac{b}{2}$	$1.000\frac{b}{2}$	60°	60°	.4000	.389	.82	---	4
C	Solid split flaps	Bomber model wing	.64c	.64c	.117c	.117c	$.275\frac{b}{2}$	$.335\frac{b}{2}$	48°	54°	.0563	.083	.96	---	-
D	Twelve small split flaps	Rectangular wing	.86c	.86c	.144c	.125c	$.300\frac{b}{2}$	$.300\frac{b}{2}$	60°	60°	.0805	.072	.89	---	5
D	Twelve small split flaps	Rectangular wing	.63c	.63c	.102c	.108c	$.300\frac{b}{2}$	$.300\frac{b}{2}$	60°	60°	.0618	.097	1.58	---	5
E	Solid split flaps	Bomber model wing	None	.76c	---	.240c	---	$.515\frac{b}{2}$	---	60°	.1450	.093	.64	---	-
F	Solid spoilers	Elliptical wing	.16c	.16c	[e] .043c_r	.058c_r	$.125\frac{b}{2}$	$.128\frac{b}{2}$	90°	90°	.0165	.041	2.48	No gap (See fig. 6)	6
G	Solid spoilers	Elliptical wing	None	.16c	---	.053c_r	---	$.244\frac{b}{2}$	---	90°	.0165	.051	3.09	No gap	6
G	Solid spoilers	Elliptical wing	None	.16c	---	.071c_r	---	$.244\frac{b}{2}$	---	90°	.0220	.051	2.32	Gap = 0.25c_B	6
G	Solid spoilers	Elliptical wing	None	.16c	---	.106c_r	---	$.244\frac{b}{2}$	---	90°	.0330	.040	1.21	Gap = 0.50c_B	6
G	Solid spoilers	Elliptical wing	None	.30c	---	.072c_r	---	$.350\frac{b}{2}$	---	90°	.0320	.066	2.06	No gap	6
G	Solid spoilers	Elliptical wing	None	.30c	---	.096c_r	---	$.350\frac{b}{2}$	---	90°	.0430	.069	1.60	Gap = 0.25c_B	6
G	Solid spoilers	Elliptical wing	None	.30c	---	.145c_r	---	$.350\frac{b}{2}$	---	90°	.0640	.063	.98	Gap = 0.50c_B	6
H	Solid spoiler	Rectangular wing	None	.20c	---	.067$\bar{c}$	---	$1.000\frac{b}{2}$	---	90°	.0667	.114	1.71	No gap	6
I	Solid spoiler	Fighter model wing	.20c	None	.165c	---	$.202\frac{b}{2}$	---	90°	---	.0342	.069	2.02	Gap = 0.33c_B	-
I	Solid spoiler	Fighter model wing	None	.20c	---	.165c	---	$.202\frac{b}{2}$	---	90°	.0342	.052	1.52	Gap = 0.33c_B	-
I	Solid spoiler	Fighter model wing	.30c	None	.165c	---	$.202\frac{b}{2}$	---	90°	---	.0342	.057	1.67	Gap = 0.33c_B	-
I	Solid spoiler	Fighter model wing	None	.30c	---	.165c	---	$.202\frac{b}{2}$	---	90°	.0342	.044	1.29	Gap = 0.33c_B	-
J	Solid spoiler	Tapered wing	.75c	None	.080c	---	$.409\frac{b}{2}$	---	90°	---	.0137	.020	1.46	No gap	7
J	Solid spoiler	Tapered wing	.75c	.75c	.080c	.080c	$.409\frac{b}{2}$	$.409\frac{b}{2}$	90°	90°	.0274	.038	1.39	No gap	7
K	Perforated plate	Fighter model wing	.63c	None	.250c	---	$.479\frac{b}{2}$	---	90°	---	.1180	.143	1.21	Gap = 0.16c_B	-
L	Double bars gap and slot	Tapered wing	.56c	None	.098c	---	$.143\frac{b}{2}$	---	90°	---	.0131	.012	.92	Gap = 0.34c_B	-
L	Double bars gap and slot	Tapered wing	None	.56c	---	.092c	---	$.143\frac{b}{2}$	---	90°	.0125	.015	1.20	Gap = 0.38c_B	-
M	Spoiler with vertical slots	Tapered wing	.56c	None	.098c	---	$.143\frac{b}{2}$	---	90°	---	.0131	.009	.69	Gap = 0.34c_B	-
M	Spoiler with vertical slots	Tapered wing	None	.56c	---	.092c	---	$.143\frac{b}{2}$	---	90°	.0125	.011	.88	Gap = 0.38c_B	-
N	Picket-fence-type brake	Bomber model wing	---	---	---	---	$.163\frac{b}{2}$	$.163\frac{b}{2}$	92°	92°	.1520	.042	.34	---	-
O	Fuselage air brakes	Bomber fuselage aft of wing	---	---	---	---	---	---	---	90°	.0444	.046	1.04	---	-
P	Fuselage dive-recovery brake	Bottom of a fighter fuselage	---	---	---	---	---	---	---	80°	.0536	.033	.62	---	-
Q	Fuselage air brakes	Bomber fuselage	---	---	---	---	---	---	---	60°	.0570	.041	.72	---	-
R	Fuselage side brakes	Side of fighter fuselage	---	---	---	---	---	---	---	89°	.0518	.053	1.02	---	-

[a] Data are for zero lift; Mach number less than 0.3.

[b] See figure 6.

[c] c = local chord of wing.

[d] $\bar{c}$ = wing chord at mean spanwise station of brake.

[e] c_r = root chord of wing.

[f] porosity: upper surface, 0.306; lower surface, 0.433.

TABLE II.– CALCULATION OF THE VARIATIONS OF AIRSPEED WITH TIME FOR AN AIRPLANE IN A 60° DIVE FROM AN ALTITUDE OF 25,000 FEET. WING LOADING, 50 POUNDS PER SQUARE FOOT

t (sec)	Δt (sec)	V_e (ft/sec)	$\bar{V}_e$ (ft/sec)	Δh (ft)	h (ft)	C_{D_n}	a/g	a (ft/sec^2)	$\bar{a}$ (ft/sec^2)	ΔV (ft/sec)	V (ft/sec)
0	0	--	--	--	25,000	0.114	0.27	8.7	--	--	700
1	1	709	704	-610	24,390	.114	.24	7.7	8.0	8.0	708
2	1	715	712	-620	23,770	.114	.20	6.4	7.0	7.0	715
4	2	725	720	-1240	22,530	.114	.17	5.5	6.0	12.0	727
6	2	737	732	-1270	21,260	.114	.13	4.2	4.9	9.8	737
8	2	744	740	-1280	19,980	.114	.07	2.3	3.2	6.4	743
10	2	746	744	-1290	18,690	.114	.03	1.0	1.6	3.2	746
14	4	745	745	-2580	16,110	.114	-.04	-1.3	-0.1	-0.4	746
18	4	736	741	-2570	13,540	.114	-.11	-3.5	-2.4	-9.6	736

Example calculation:

An airplane in a 60° dive at a speed of 700 feet per second instantaneously extends air brakes at time $t = 0$.

Drag coefficient of airplane without air brakes, $C_D = 0.014$.

Drag increment due to air brakes, $\Delta C_D = 0.100$.

At $t = 0$

$h = 25{,}000$ ft

$a/g = 0.27$ (See guide lines, fig. 1)

$a_o = (0.27)(32.2) = 8.7$ ft/sec^2

$t = 1$ sec

$\Delta t_1 = 1$ sec

$V_e = 700 + 8.7(1) = 709$ ft/sec

$\bar{V}_e = \frac{1}{2}(700 + 709) = 704$ ft/sec

$\Delta h = \bar{V}_e \Delta t \sin\gamma = (704)(1)(-0.866) = -610$ ft

$h = 25{,}000 - 610 = 24{,}390$ ft

$a/g = 0.24$ (fig. 1)

$a_1 = (0.24)(32.2) = 7.7$ ft/sec^2

$\bar{a} = \frac{1}{2}(8.7 + 7.7) = 8.2$ ft/sec^2

$\Delta V = \bar{a}\,\Delta t = 8.2$ ft/sec

$V = 700 + 8 = 708$ ft/sec

$t = 2$ sec

$\Delta t_2 = 1$ sec

$$V_e = V + \Delta t_2 \left[a_1 + \frac{(a_1 - a_o)}{2} \frac{\Delta t_2}{\Delta t_1} \right]$$

$$= 708 + (1)\left[7.7 + \frac{7.7 - 8.7}{2} \frac{(1)}{(1)} \right]$$

TABLE III.– CALCULATION OF VARIATIONS WITH TIME OF AIRSPEED AND FLIGHT-PATH ANGLE FOR AN AIRPLANE ENTERING A 60° DIVE. WING LOADING, 50 POUNDS PER SQUARE FOOT. INITIAL ALTITUDE, 25,000 FEET

t (sec)	Δt (sec)	V_e (ft/sec)	$\bar{V}_e$ (ft/sec)	n	$\bar{\gamma}$ (deg)	$\Delta\gamma$ (deg)	γ (deg)	$\frac{r}{1000}$ (ft)	Δh (ft)	h (ft)	q_e (lb/sq ft)	C_L	C_{D_n}	a/g	a (ft/sec²)	$\bar{a}$ (ft/sec²)	$\Delta\bar{V}$ (ft/sec)	V (ft/sec)
0	0	--	--	1	---	---	0	--	---	25,000	261	0.19	0.015	-0.08	-2.6	---	---	700
1	1	689	695	-1.5	-3.2	-6.5	-6.5	6.0	-30	24,970	253	-.30	.118	-.50	-16.2	-9.2	-9.2	691
1	1	691	696	-1.5	-3.3	-6.6	-6.6	6.0	-30	24,970	255	-.29	.118	-.48	-15.5	-8.9	-8.9	691
2	1	679	685	-1.5	-9.9	-6.7	-13.3	6.0	-60	24,910	246	-.30	.118	-.35	-11.3	-13.4	-13.4	678
3	1	669	674	-1.5	-16.6	-6.6	-19.9	5.9	-180	24,730	241	-.31	.118	-.22	-7.1	-9.2	-9.2	669
4	1	663	666	-1.5	-23.2	-6.6	-26.5	5.7	-260	24,470	238	-.32	.118	-.10	-3.2	-5.1	-5.1	664
6	2	664	664	-1.5	-33.0	-13.0	-39.5	5.9	-570	23,900	245	-.30	.118	.06	1.9	-0.6	-1.2	663
8	2	670	666	-1.5	-45.7	-12.0	-51.5	6.1	-770	23,130	256	-.29	.118	.20	6.4	4.1	8.2	671
[a]9.5	1.5	682	676	-1.5	-55.7	-8.5	-60.0	6.7	-840	22,290	272	-.28	.118	.23	7.4	6.9	10.3	681
12	2.5	700	690	[b].5	-60.0	0	-60.0	∞	[c]-1490	20,800	298	.08	.113	.18	5.8	6.6	16.5	698
15	3	712	705	.5	-60.0	0	-60.0	∞	-1830	18,970	332	.08	.113	.09	2.9	4.3	12.9	711

[a] $\Delta\gamma = -60.0 + 51.5 = -8.5°$. $\bar{\gamma} = -51.5 - \frac{8.2}{2} = -55.7°$. $\Delta t = 1.5$ sec (figs. 5(c) and (d) for $V_e = 670$ ft/sec)

[b] Normal acceleration factor for a steady 60° dive, $n = \cos(-60°) = 0.5$

[c] $\Delta h = \bar{V}_e \Delta t \sin(-60°)$

Example calculation:

An airplane begins a dive from level flight at 700 feet per second, reaching an indicated normal acceleration of -1.5g during the first second, and maintaining this acceleration until the dive angle is 60°.

Net drag coefficient of the airplane, $C_{D_n} = 0.013 + 0.060\, C_L^2 + \Delta C_D$

Drag increment due to air brakes, $\Delta C_D = 0.100$

At $t = 0$

$\gamma = 0$, Proceeding as in the case of constant γ (table II), $a/g = -0.08$, $a = -2.6$ ft/sec²

$t = 1$ sec

$\bar{a}$ is estimated, considering that $C_D = 0.015$ at $t = 0$ and $C_D = 0.118$ at $t = 1.0$, $\bar{a}_e = -11$ ft/sec²

$V_e = 700 - 11\ (\Delta t) = 689$ ft/sec ($\Delta t = 1$ sec)

$n = -1.5$

$n = \cos\gamma = -2.5$, for $\bar{\gamma} = 0°$ (fig. 5(a))

$\gamma_e = 1/2\ \Delta\gamma = 1/2\ (6.5) = 3.2°$ (figs. 5(c) and (d). This may possibly require more than than a single trial in some instances.)

$\Delta\gamma = -6.5°$ (figs. 5(a), (b), and (c))

$r/1000 = 6.0$ (See guide lines, for example 1, figs. 5(a) and (b))

$\Delta h = -30$ ft (figs. 5(e) and (f) Minus sign chosen because a dive has been specified)

$h = 25{,}000 - 30 = 24{,}970$ ft

$q_e = 1/2\ \rho V_e^2 = 253$ lb/sq ft

$C_L = \frac{(-1.5)\ (50)}{253} = -0.30$

$a/g = -0.50$ (fig. 1)

$V = 700 - \frac{32.2}{2}\ (-0.08 - 0.50)\ (1) = 691$ ft/sec

To show that the original estimate was close enough to give the correct velocity, the calculations have been repeated in the table with $V_e = 691$ ft/sec. This again gives $V = 691$ ft/sec.

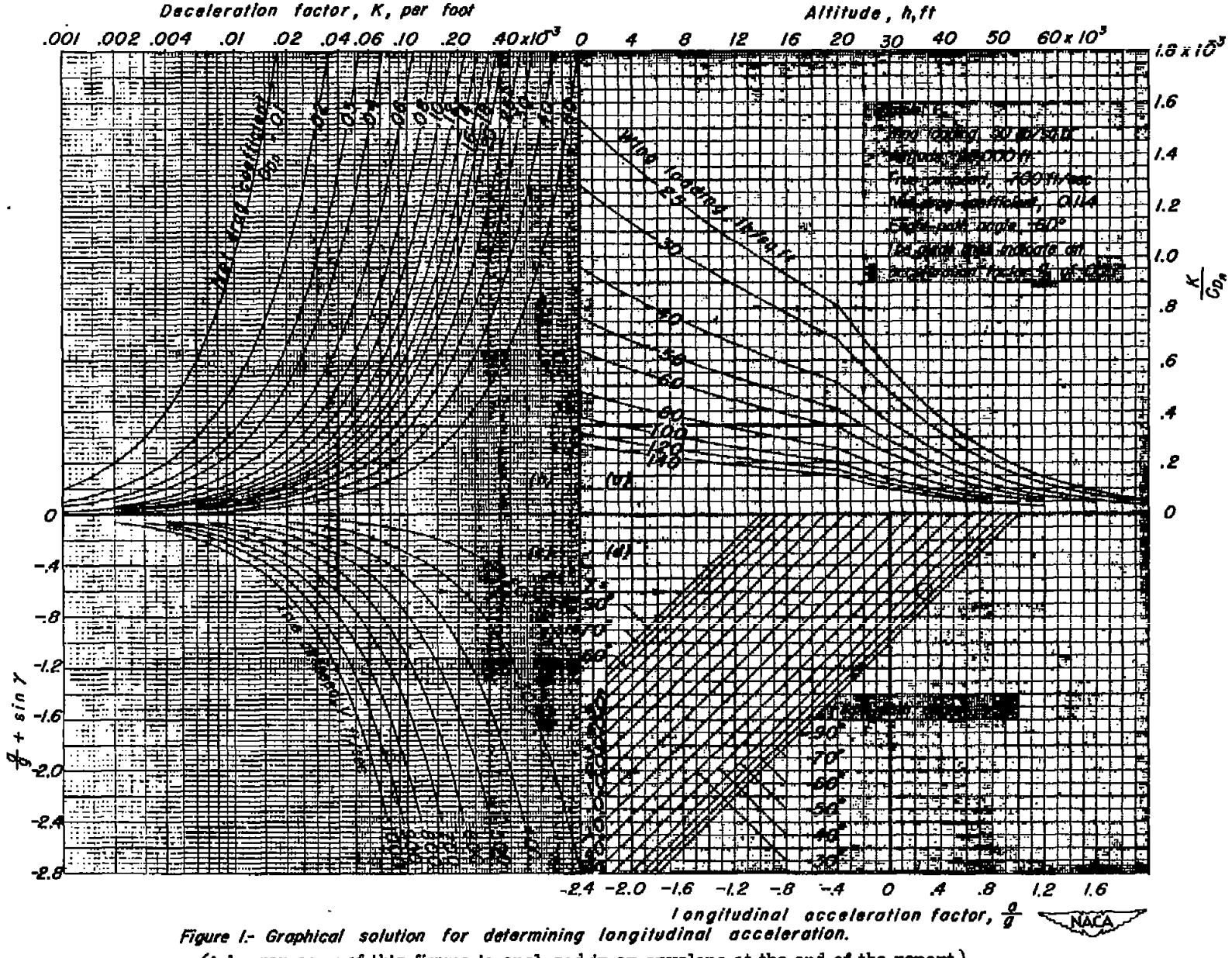

Figure 1.- Graphical solution for determining longitudinal acceleration.

(A larger copy of this figure is enclosed in an envelope at the end of the report.)

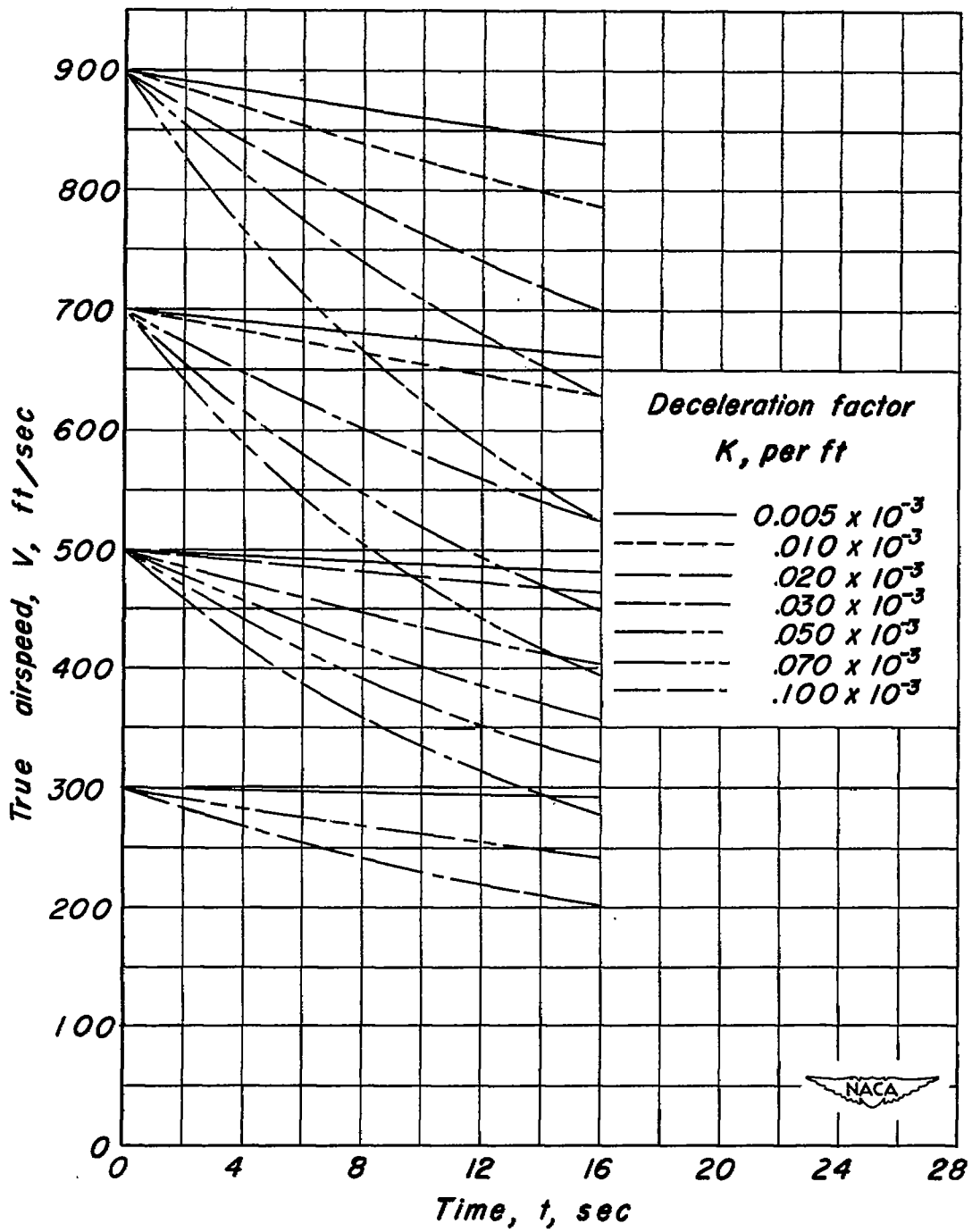

Figure 2.— The effect of deceleration factor K upon the variation of speed with time for several initial speeds. Level flight condition.

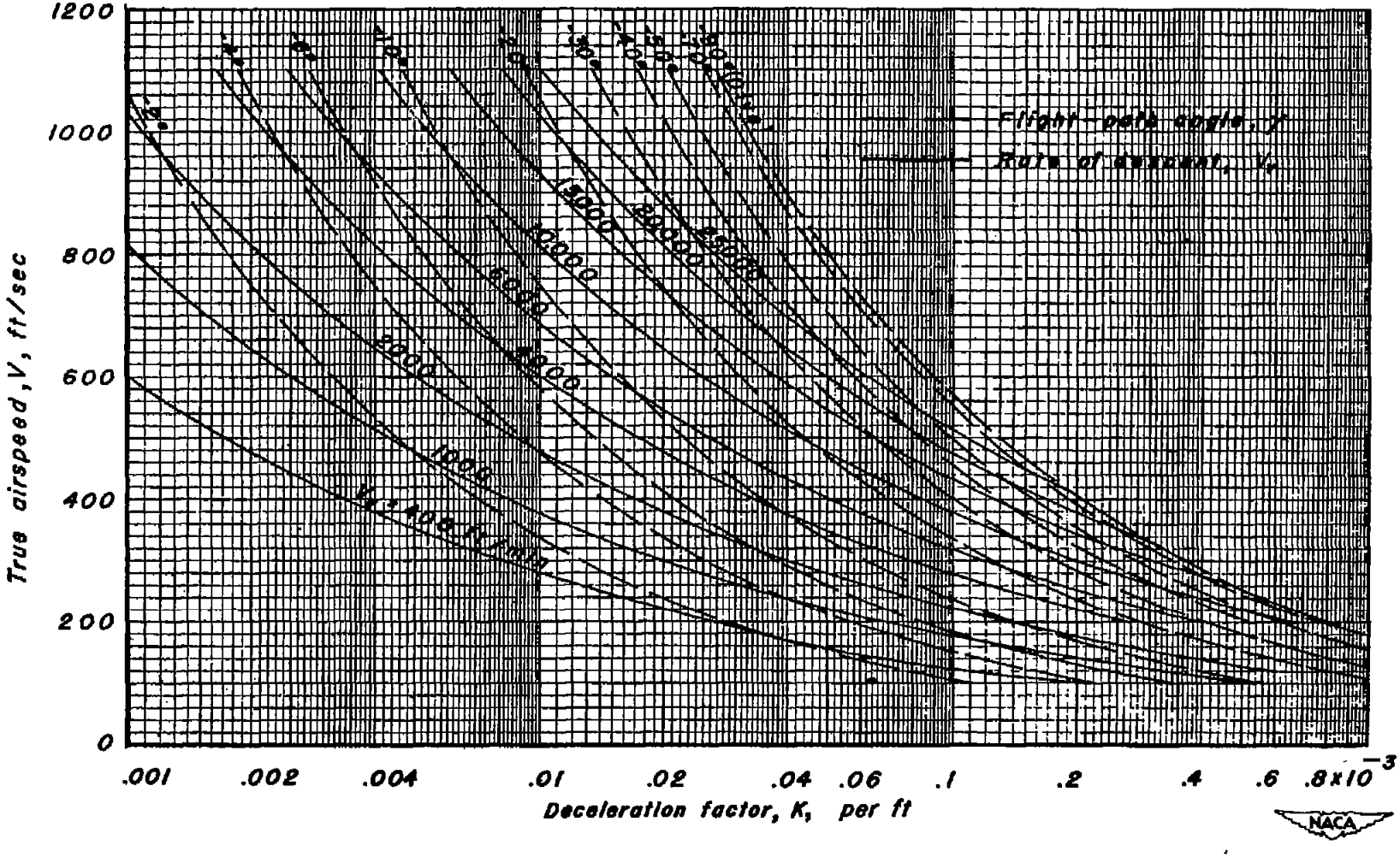

Figure 3.— Effect of deceleration factor, K, upon the vertical speed and the flight-path angle for constant-speed descent.

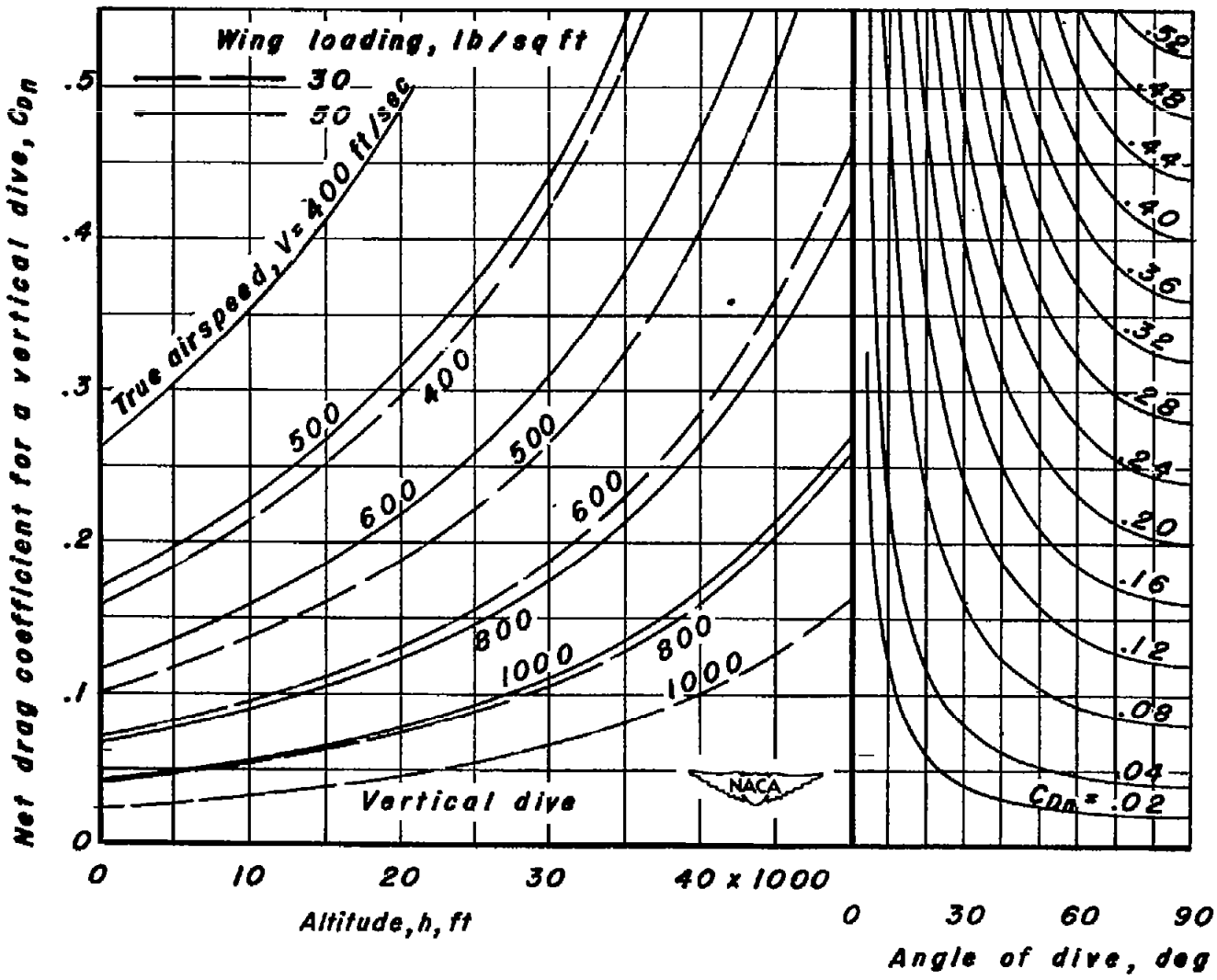

Figure 4. — Drag coefficient required for no longitudinal acceleration in a dive.

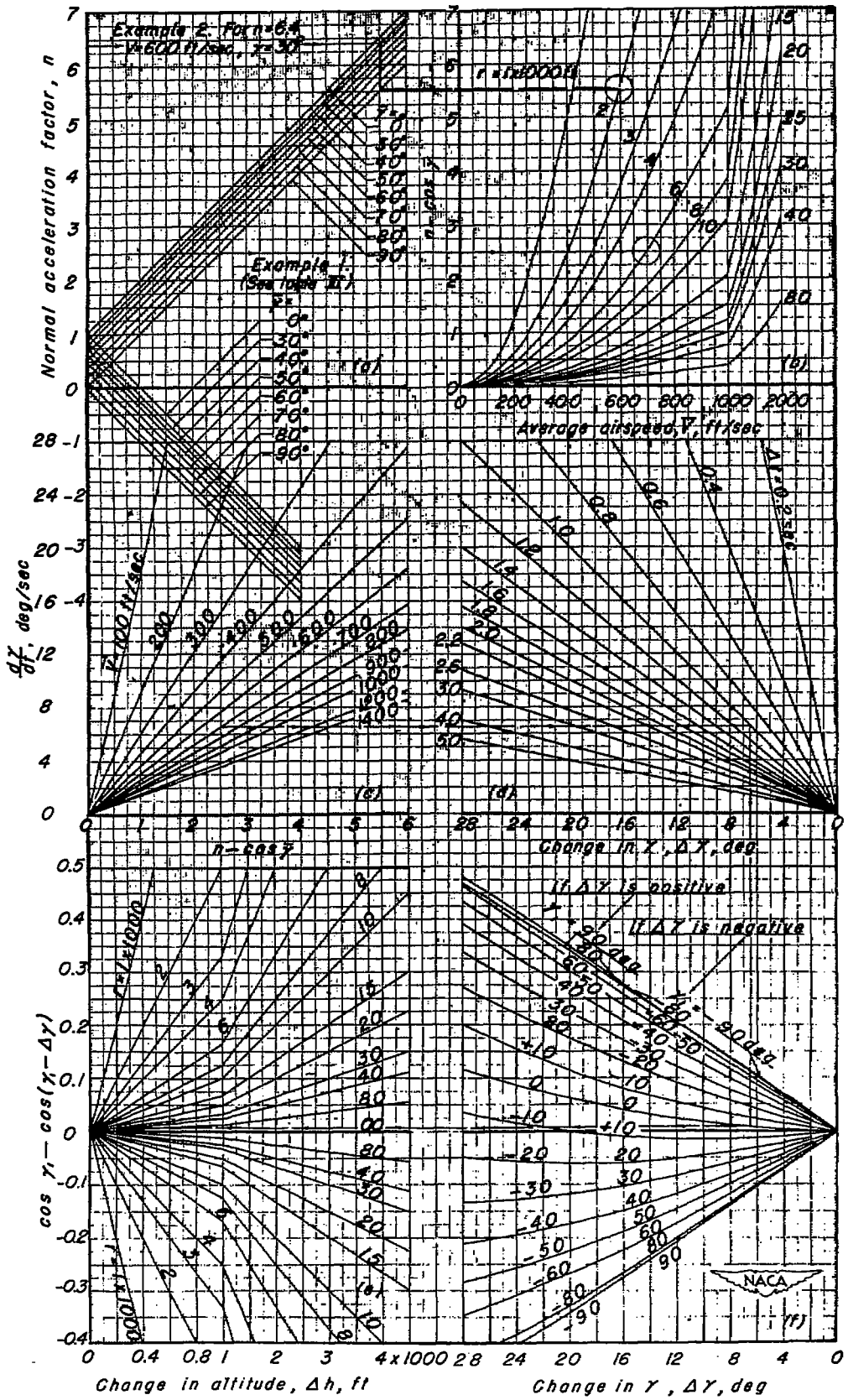

Figure 5.— Graphical solution for changes of altitude and flight-path angle.
(A larger copy of this figure is enclosed in an envelope at the end of the report.)

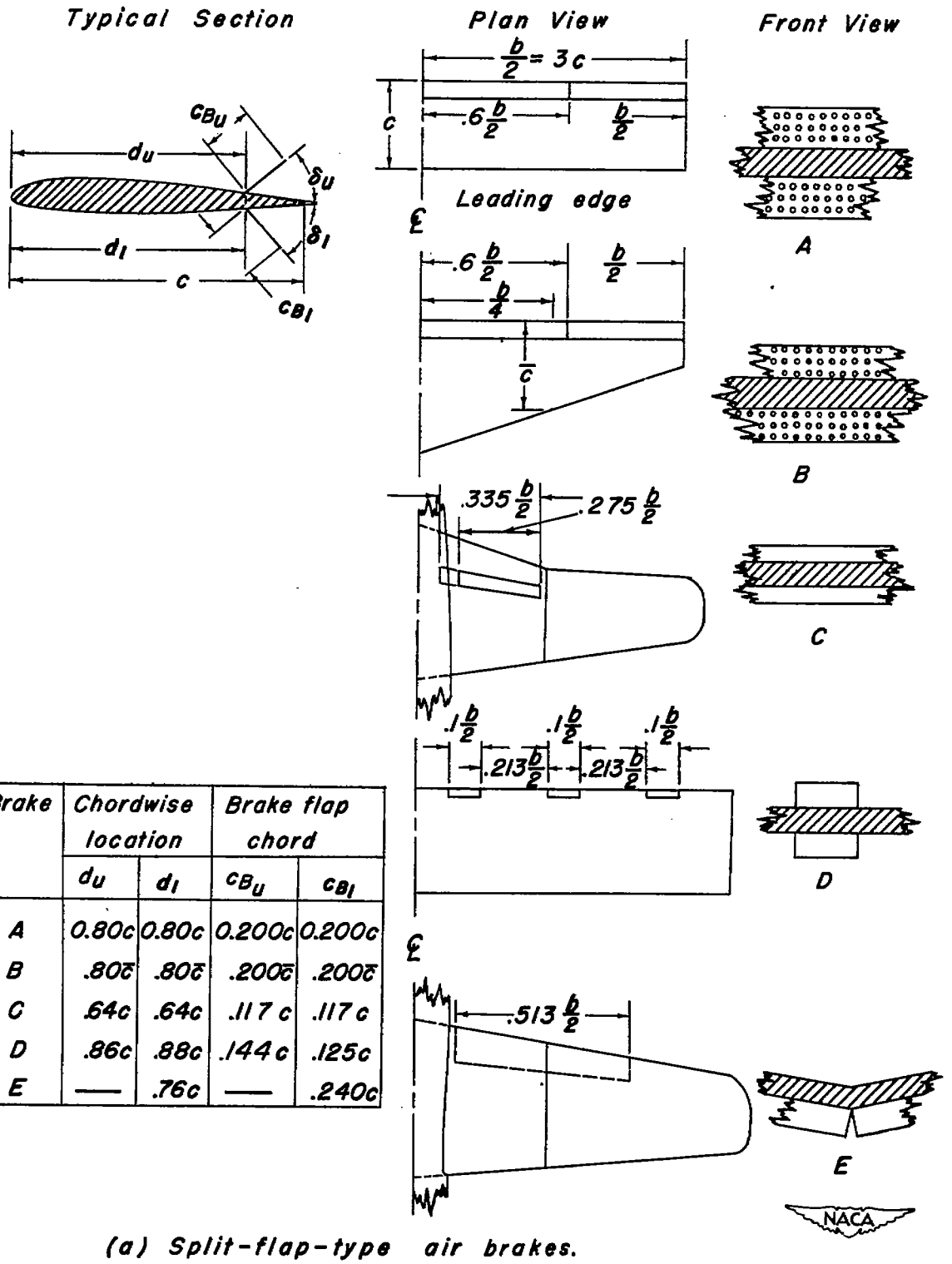

Brake	Chordwise location		Brake flap chord	
	d_u	d_l	c_{B_u}	c_{B_l}
A	0.80c	0.80c	0.200c	0.200c
B	.80$\bar{c}$	.80$\bar{c}$	.200$\bar{c}$	.200$\bar{c}$
C	.64c	.64c	.117 c	.117 c
D	.86c	.88c	.144 c	.125c
E	—	.76c	—	.240c

(a) Split-flap-type air brakes.

Figure 6.— Aerodynamic brake installations for which drag characteristics are summarized in Table I.

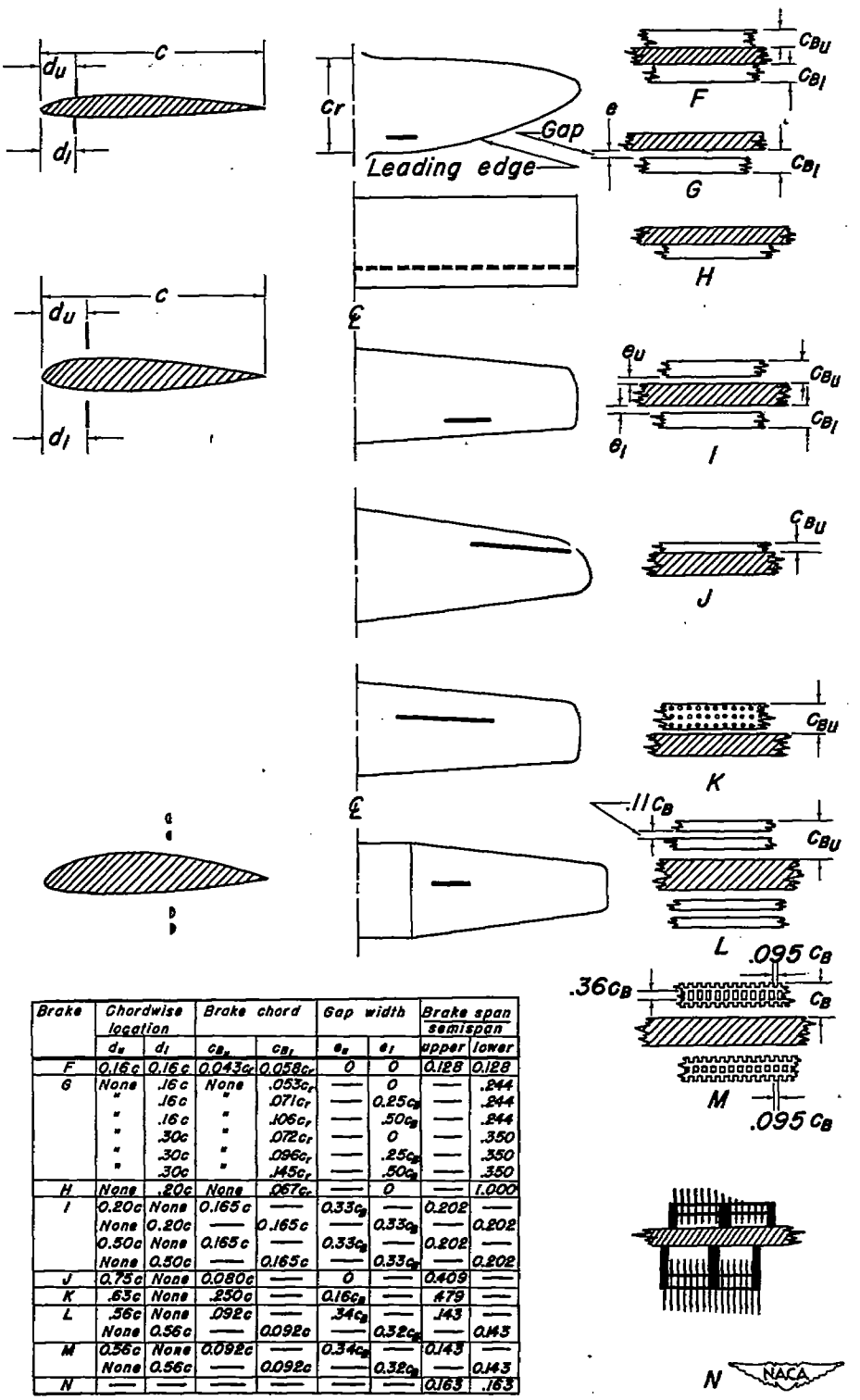

Brake	Chordwise location		Brake chord		Gap width		Brake span semispan	
	d_u	d_l	c_{B_u}	c_{B_l}	e_u	e_l	upper	lower
F	0.16c	0.16c	$0.043c_r$	$0.058c_r$	0	0	0.128	0.128
G	None	.16c	None	$.053c_r$	—	0	—	.244
	"	.16c	"	$.071c_r$	—	$0.25c_{B_l}$	—	.244
	"	.16c	"	$.106c_r$	—	$.50c_{B_l}$	—	.244
	"	.30c	"	$.072c_r$	—	0	—	.350
	"	.30c	"	$.096c_r$	—	$.25c_{B_l}$	—	.350
	"	.30c	"	$.145c_r$	—	$.50c_{B_l}$	—	.350
H	None	.20c	None	$.067c_r$	—	0	—	1.000
I	0.20c	None	0.165c	—	$0.33c_{B_u}$	—	0.202	—
	None	0.20c	—	0.165c	—	$0.33c_{B_l}$	—	0.202
	0.50c	None	0.165c	—	$0.33c_{B_u}$	—	0.202	—
	None	0.50c	—	0.165c	—	$0.33c_{B_l}$	—	0.202
J	0.75c	None	0.080c	—	0	—	0.409	—
K	.63c	None	.250c	—	$0.16c_{B_u}$	—	.479	—
L	.56c	None	.092c	—	$.34c_{B_u}$	—	.143	—
	None	0.56c	—	0.092c	—	$0.32c_{B_l}$	—	0.143
M	0.56c	None	0.092c	—	$0.34c_{B_u}$	—	0.143	—
	None	0.56c	—	0.092c	—	$0.32c_{B_l}$	—	0.143
N	—	—	—	—	—	—	0.163	.163

(b) Spoiler- and picket-fence-type air brakes.

Figure 6. — Continued.

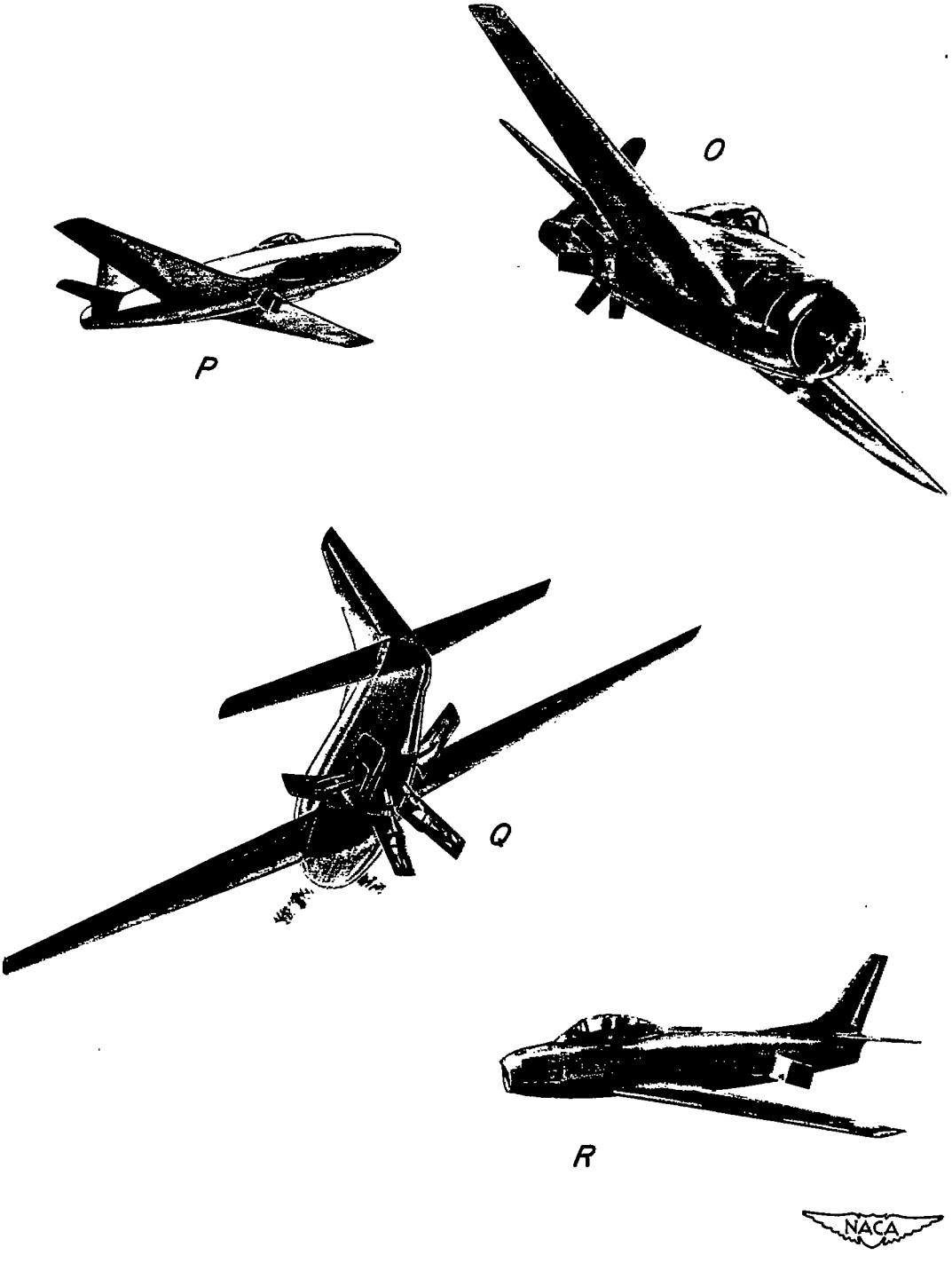

(c) Fuselage air brakes.

Figure 6.— Concluded.

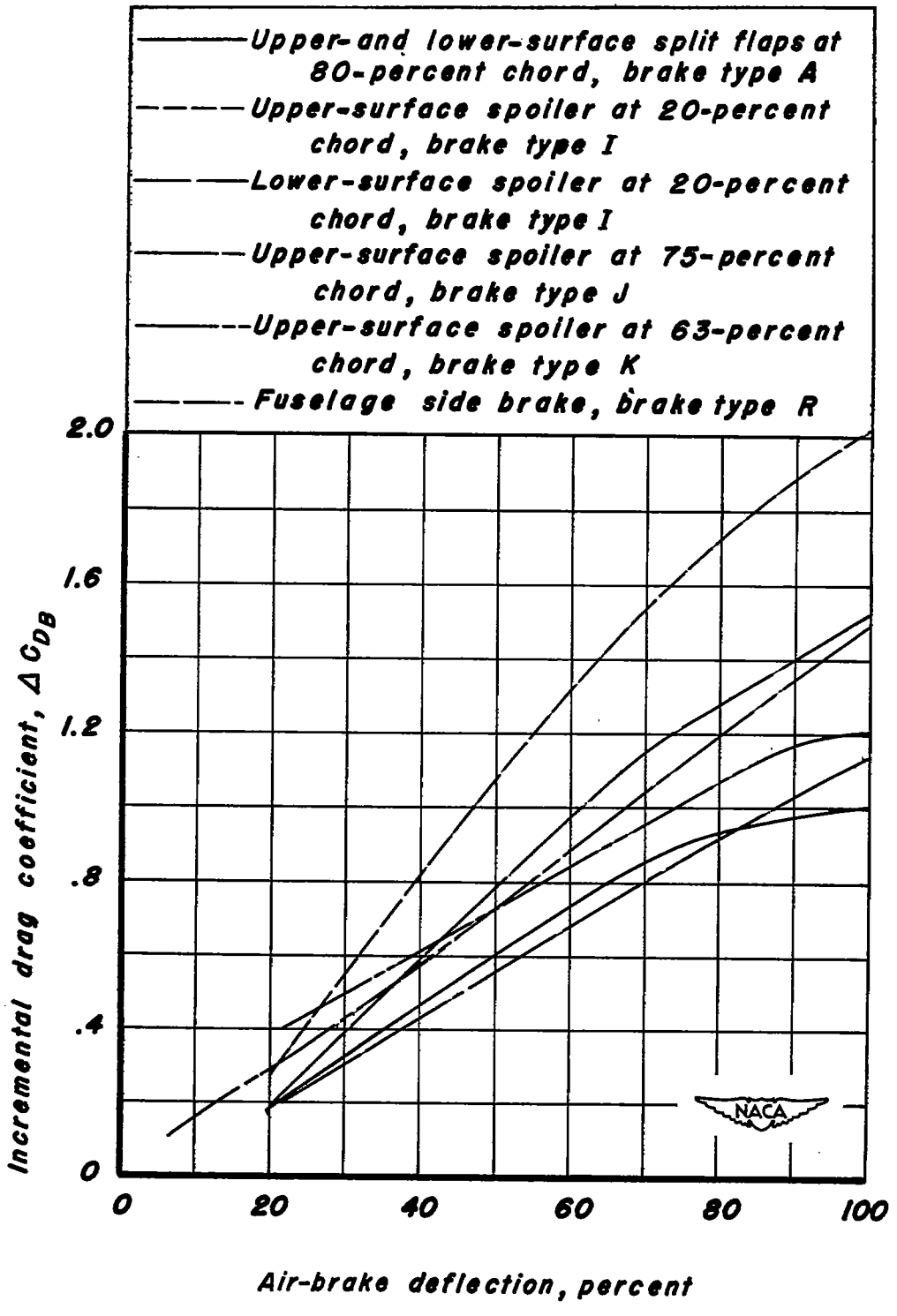

Figure 7.— The variation of air-brake drag coefficient with percent of full brake deflection.

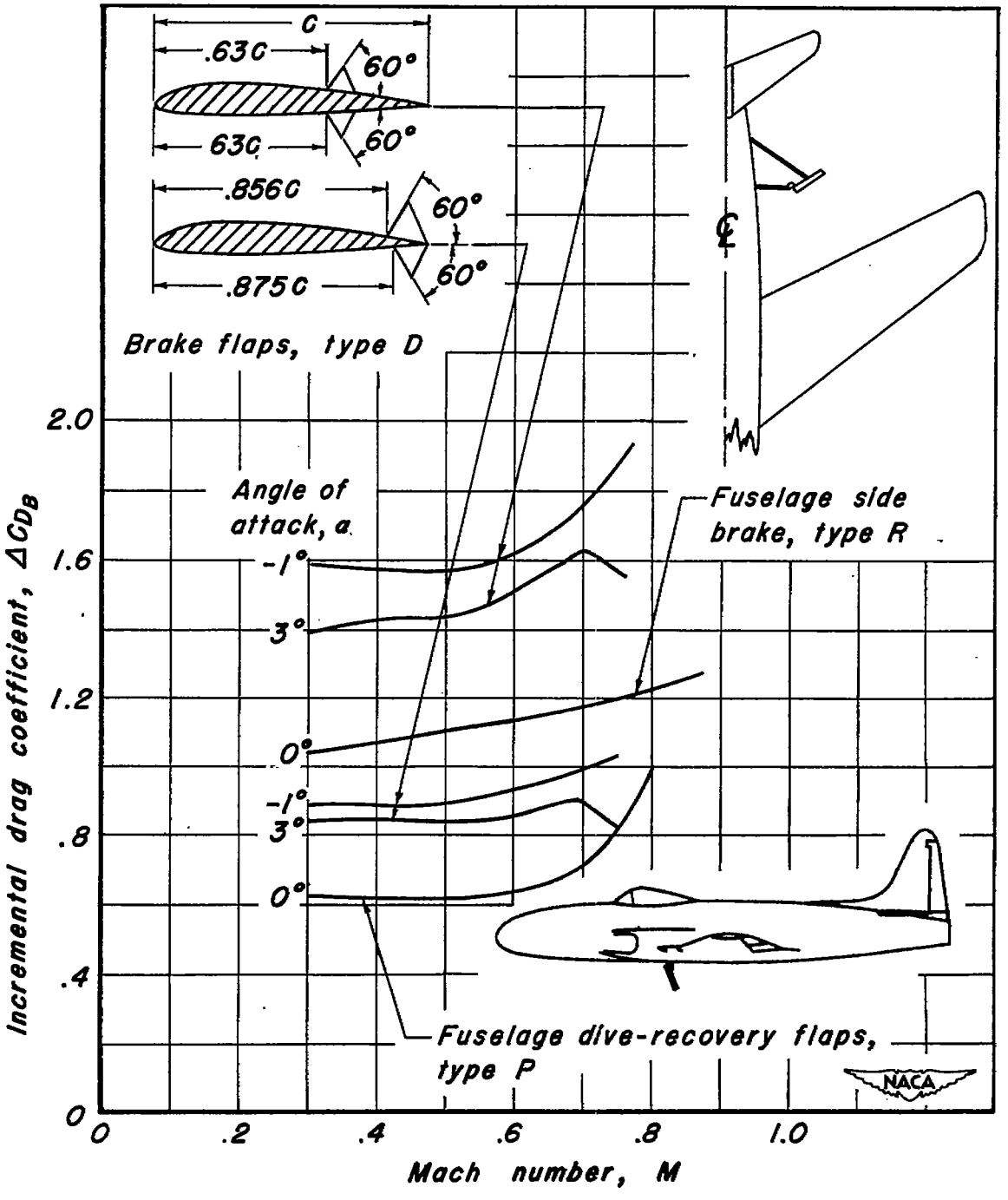

Figure 8.— Effect of Mach number on the incremental drag coefficient due to air brakes.

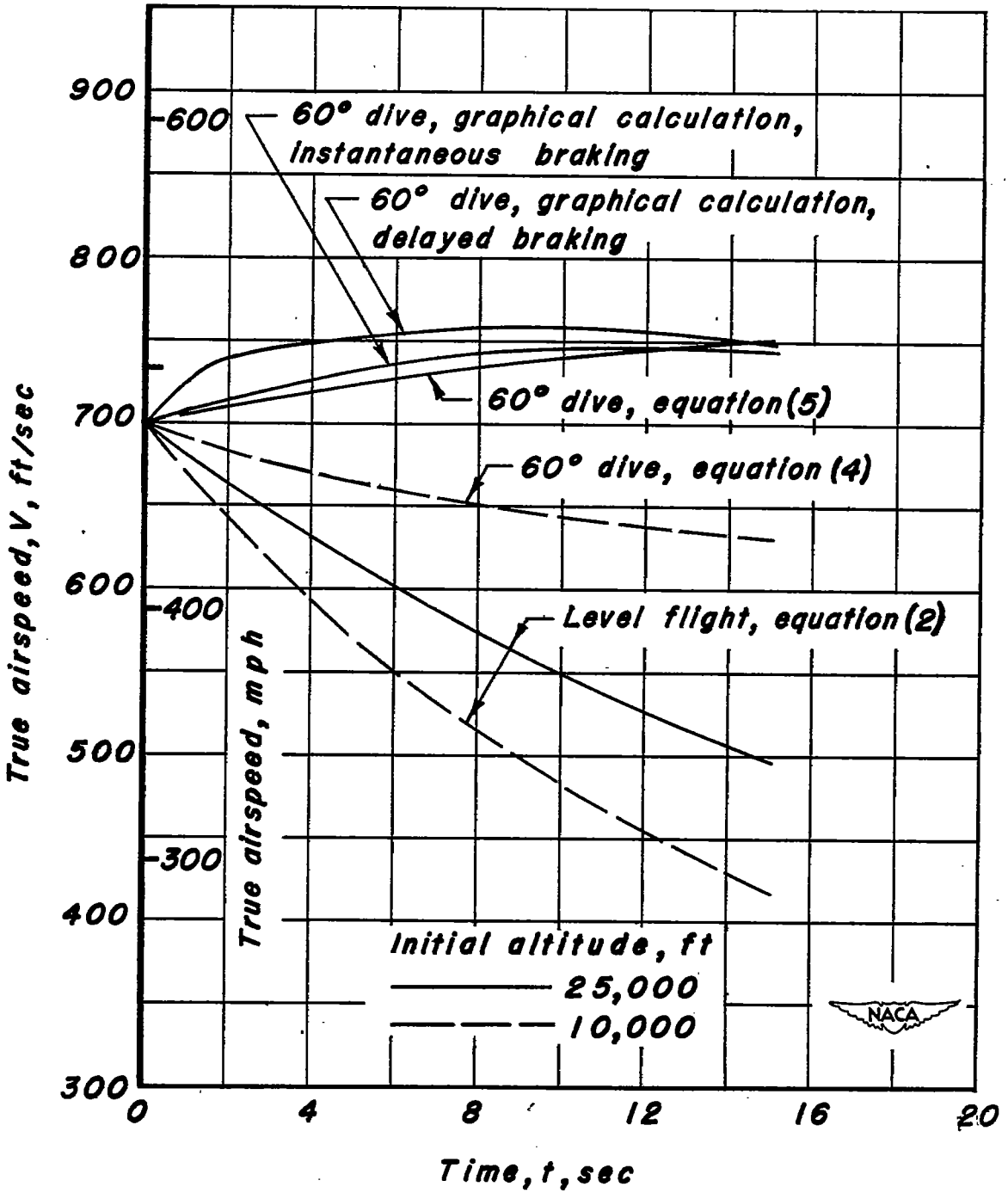

Figure 9.— Variation of airspeed with time for an airplane with aerodynamic brakes. Wing loading, 50 lb/sq ft.

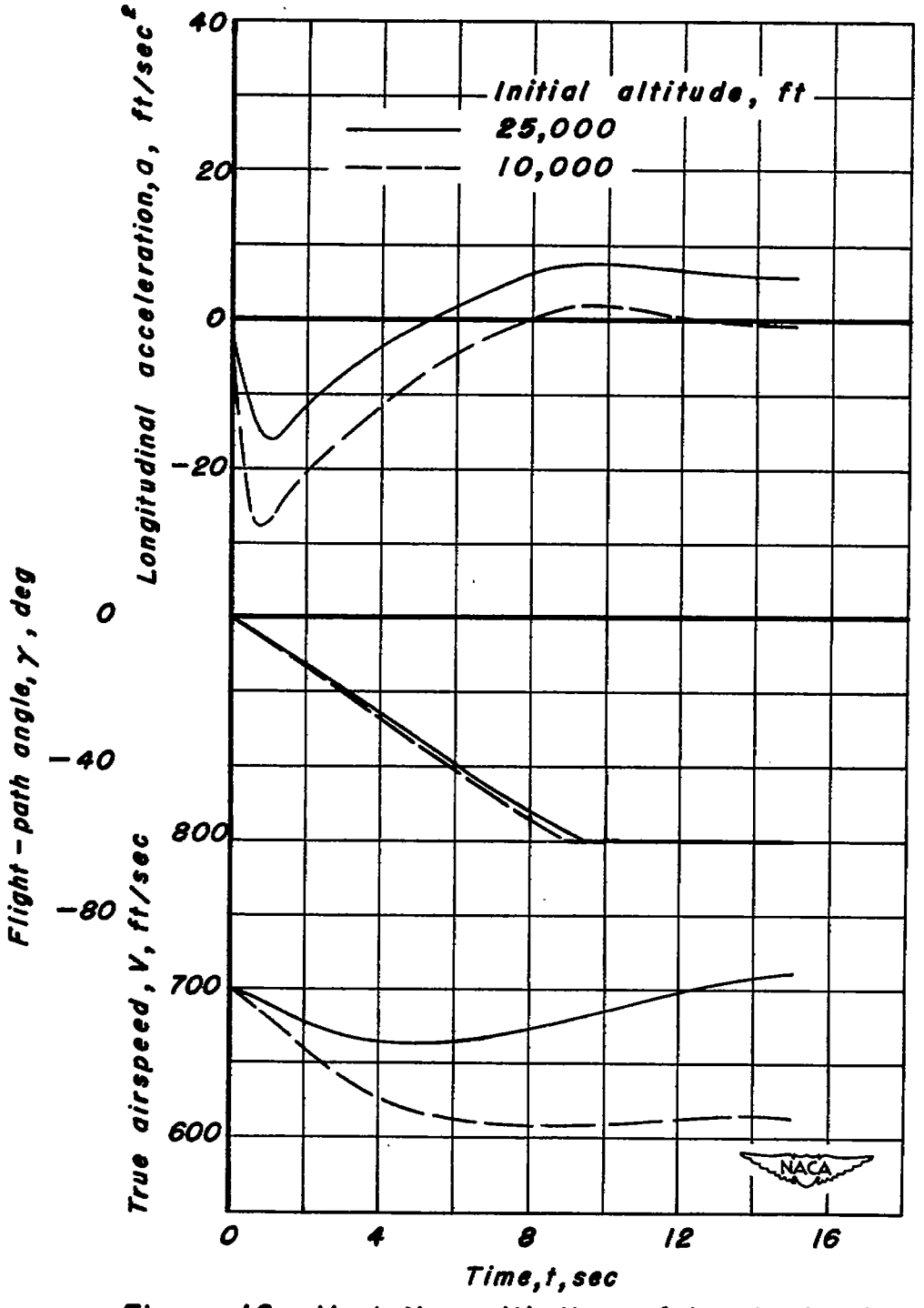

Figure 10.— Variation with time of longitudinal acceleration, flight-path angle, and airspeed of an airplane entering a 60° dive. Wing loading, 50 lb/sq ft.

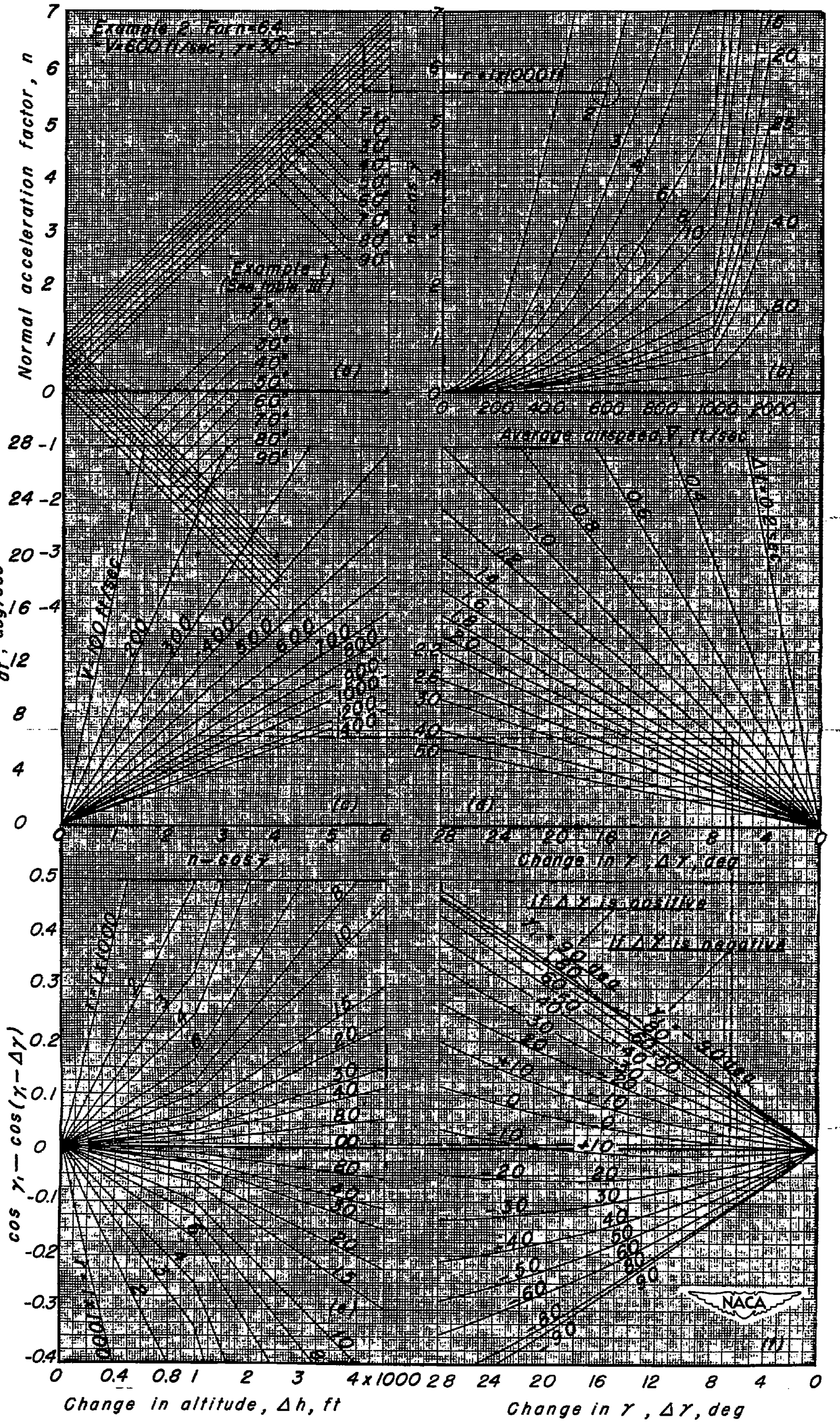

Figure 5.— Graphical solution for changes of altitude and flight-path angle.

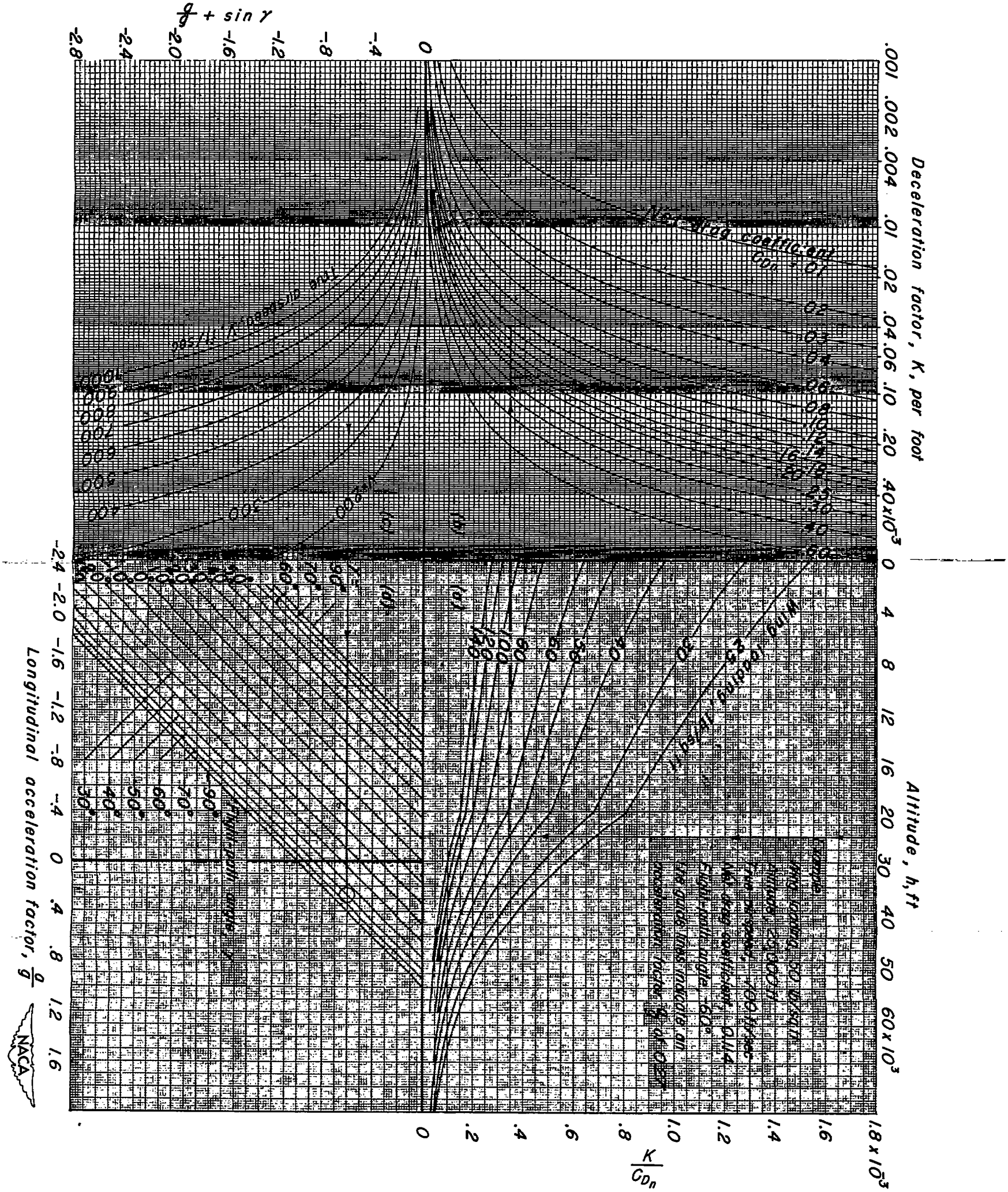

Figure I.- Graphical solution for determining longitudinal acceleration.

NACA-Langley - 9-1-49 - 950